Analyst

PAPER

View Article Online
View Journal | View Issue

Cite this: *Analyst*, 2015, **140**, 1894

Extremely supercharged proteins in mass spectrometry: profiling the pH of electrospray generated droplets, narrowing charge state distributions, and increasing ion fragmentation†

Muhammad A. Zenaidee and William A. Donald*

The effects of 12 acids, 4 solvents, and 8 low-volatility additives that increase analyte charging (*i.e.*, superchargers) on the charge state distributions (CSDs) of protein ions in ESI-MS were investigated. We discovered that (i) relatively low concentrations [5% (v/v)] of 1,2-butylene carbonate (and 4-vinyl-1,3-dioxolan-2-one) can be added to ESI solutions to form higher charge states of cytochrome *c* and myoglobin ions than by using more traditional additives (*e.g.*, propylene carbonate, sulfolane, or *m*-nitrobenzyl alcohol) under these conditions and (ii) the width of CSDs narrow as the effectiveness of superchargers increase, which concentrates protein ions into fewer detection channels. The use of strong acids (pK_a values < 0) results in essentially no protein supercharging, higher adduction of acid molecules, and wider CSDs for many superchargers and proteins, whereas the use of weak acids (pK_a > 0) results in significantly higher protein ion charging, less acid adduction, and narrower CSDs, indicating that protein ion supercharging in ESI can be significantly limited by the binding of conjugate base anions of acids that neutralize charge sites and broaden CSDs. The extent of protein charging as a function of acid identity (HA) does not strongly correlate with gas-phase proton transfer data (*i.e.*, gas-phase basicity and proton affinity values for HA and A^-), solution-phase protein secondary structures (as determined by circular dichroism spectroscopy), and/or acid molecule volatility data. For protein-denaturing solutions, these data were used to infer that the "effective" pH of ESI generated droplets near the moment of ion formation can be ~0, which is *ca.* 1 to 3 pH units lower than the pH of the solutions prior to ESI. Electron capture dissociation (ECD) of [ubiquitin, 17H]$^{17+}$ resulted in the identification of 223 cleavages, 74 of 75 inter-residue sites, and 92% ECD fragmentation efficiency, which correspond to highest of these values that have been obtained by ECD of a single isolated charge state of ubiquitin.

Received 19th December 2014,
Accepted 25th January 2015

DOI: 10.1039/c4an02338b

www.rsc.org/analyst

Introduction

Electrospray ionization (ESI) is effective for forming intact gaseous ions of proteins from solution for detection by mass spectrometry (MS).[1] A distinctive advantage of ESI is that a distribution of multiply charged ions, [M, *z*H]$^{z+}$ (charge state distributions; CSDs), can be produced that have higher charge densities than those formed using other known methods. Multiple charging extends the mass range of most mass analysers,[1] which enables protein ions to be detected using nearly any ESI mass spectrometer. Ions that have more charges tend to dissociate significantly more readily than those with fewer charges partly because charge sites often direct the bond cleavage of ions in many types of tandem-MS experiments.[2] For electron capture dissociation (ECD), the number of fragment ions,[3] the efficiency of fragmentation,[3] and the amount of energy that is deposited increases as ion charge increases,[3a,b,4] which can significantly increase the number of cleavage sites

School of Chemistry, University of New South Wales, Sydney, New South Wales 2052, Australia. E-mail: w.donald@unsw.edu.au; Fax: +61 (2) 9385 6141; Tel: +61 (2) 9385 8827

† Electronic supplementary information available: Tables S1–S5: Effects of ion source voltages and temperatures on the extent of cytochrome *c* charging, SC dipole moment and surface tension values, effects of acid concentration on the CSDs of protonated cytochrome *c*, tune conditions for ESI of different proteins, and acid volatility data. Fig. S1–S3: Extent of protonated cytochrome *c* charging plotted *vs.* GB and PA values of the acids and conjugate base anions of the acids and acid volatility data, and in order of the Hofmeister series. Fig. S4–S8: Effects of acid identity on CSDs of proteins/peptides in ESI without SCs, effects of acid identity on the W_z values for protein ions, and effects of solvent identity on the CSDs for protein ions with and without SCs. Fig. S9–S10: ESI and ECD mass spectra and corresponding relative ECD-MS fragment ion abundances at each inter-amino acid residue site for isolated [ubiquitin, 13H]$^{13+}$ and [ubiquitin, 17H]$^{17+}$. Full methodological details and an extended discussion of Hofmeister effects are given. See DOI: 10.1039/c4an02338b

and the resulting sequence coverage. ESI solutions that denature proteins are often used to ensure the formation of protein ions in elongated conformations that hold significantly more charge than those that are compact.[5] However, the widths of protein CSDs increase significantly as the size of proteins increase, which reduces signal-to-noise ratios (S/N) by distributing signal over more detection channels and "clutters" mass spectra.[6] The S/N for protein ions formed from denaturing solutions decrease exponentially as protein sizes increase owing solely to CSD broadening.[6] Thus, it would be useful to (i) narrow protein CSDs and (ii) shift charge states to low m/z values where many MS instruments excel.

The dynamic processes that occur during ESI are complex and many factors affect protein CSDs (*e.g.*, pH,[7] conformation,[5,7] proton transfer reactivity,[8] and surface tension).[9] In ESI, a potential is applied to a solution flowing through a capillary, which results in the emission of a fine mist of charged droplets.[1] The surface charge density of the droplets increases as relatively volatile components of the droplets preferentially evaporate. If sufficiently high, charge–charge repulsion can overcome the forces that hold droplets together at the Rayleigh limit,[1] in which the number of charges a droplet can accommodate scales with $\gamma^{1/2}$ (where γ is surface tension). Upon droplet fission, a stream of smaller droplets is emitted that removes a significant fraction of charge (*ca.* 10 to 50%), but relatively little mass (<5%) from the precursor.[1,10] In the charge residue model,[11] sequential evaporation/fission cycles yield a droplet containing a single ion that evaporates. In the ion evaporation model,[12] an ion desorbs from a droplet that is sufficiently charged. Over the lifespan of an ESI droplet, the vast majority of droplet mass is lost to evaporation,[1] which results in the enrichment of charge carriers (*e.g.*, H_3O^+). Based on laser-induced fluorescence measurements, the pH of positively charged droplets decrease by ≥1 pH unit during ESI,[13] which is consistent with results for the dissociation of pH sensitive metal ion complexes in ESI-MS.[14] However, the pH of ESI generated droplets that contain protein ions is not known.

In ESI, the extent that proteins are charged depends on the protein structure (*e.g.*, number of basic sites),[7,15] the solution composition,[9,16] and instrumental effects.[17] The apparent gas-phase basicity values (GB^{app}, which include the repulsive Coulomb barrier to proton transfer) of protein ions decrease as the charge states increase.[18] If sufficiently protonated, the GB^{app} values of protein ions approach the GB values of solvent molecules, which can result in proton transfer reactions between protein ions and residual solvent that can limit protein ion charging.[8a,18a] For example, the average charge states of cytochrome *c* (cyt *c*) ions formed from solutions containing 47/50/3% water/solvent/acetic acid (solvent = water, GB of 157.7 kcal mol^{-1}; methanol, 173.2 kcal mol^{-1}; acetonitrile, 179.0 kcal mol^{-1}; isopropanol, 182.3 kcal mol^{-1}) steadily decreased from 16.8 (water) to 15.6 (isopropanol) as the GB of the solvent increased.[8a]

The neutralization of protonation sites by the adduction of anions in ESI can also reduce analyte charging. For example, the average charge states of protonated cyt *c* ions formed by ESI from denaturing solutions can shift by up to *ca.* 15% by using different acids (*e.g.*, 14.8 *vs.* 12.5, for CH_3COOH *vs.* CCl_3COOH),[16] which indicates that the conjugate base anions of the acids can neutralize protein charge states. The binding of an anion to a protonation site reduces the charge of the protein ion by forming a neutral acid adduct ($[M, (z-1)H, HA]^{(z-1)+}$) that can be readily lost.[16] Acid/anion adduction to other biomolecules has been observed in ESI.[16,19] Although the role of anions/solvent molecules in reducing analyte charging in ESI is recognized, the reported shifts in the CSDs as a result of changing the identity of anions/solvent in ESI solutions are relatively modest (*e.g.*, ≤3 protons for cyt *c* ions).[16]

Protein ion charge states can be shifted to higher values by chemical derivatization,[20] altering ESI source conditions,[17b] and modifying the composition of ESI solutions[19a] and plumes.[21] A simple approach to form protein ions in the highest known protonation states is to add small non-volatile molecules (superchargers, SCs) that are polar and have relatively high γ values into ESI solutions.[8a,9a,22] More than a dozen SCs have been used to significantly increase the extent of analyte charging in ESI,[8a,9a,22] including *m*-nitrobenzyl alcohol (*m*-NBA)[9a] and sulfolane.[22a,23] Supercharging additives are useful for significantly increasing tandem-MS ion fragmentation efficiency and the resulting sequence coverage[24] for proteins and peptides in liquid chromatography ESI-MS experiments.[25]

Three mechanisms have been proposed for protein supercharging in ESI from denaturing solutions,[9a,23,26] in which protein conformational effects should be negligible. For all three, non-volatile supercharging additives are enriched during sequential droplet evaporation/fission cycles.[22b,27] In the surface-tension mechanism,[9a] the additives increase the droplet γ near the moment of ion formation to form more highly charged droplets than without the additive, which results in the transfer of more charge to the analyte. However, the role of γ in ESI has been questioned[22a,28] owing partly to the many factors that can affect protein ion CSDs, which makes it challenging to determine the dominant factors that are responsible for the extent of protein charging in ESI. For example, Samalikova *et al.* suggested that γ in ESI is not a significant factor based partly on the observation that protein CSDs did not shift upon use of ESI solutions that were acidified with HCl compared to acetic acid[28] because the difference in droplet γ values were predicted to be relatively large (~60%). However, the neutralization of protonation sites by the conjugate base anions of acids did not appear to be considered. In the Brønsted-acid/base mechanism,[26] the enhanced charging of analytes by the addition of SCs is attributed to protonated supercharging additives being less basic than water, which ultimately results in the formation of more highly protonated analyte molecules. In the dipole-moment based mechanism,[23] supercharging additives solvate protonation sites in mature ESI droplets, which decreases charge–charge repulsion and increases the number of charges accommodated by an analyte ion.

Recently, we discovered that by use of ethylene carbonate (EC) and propylene carbonate (PC),[29] significantly higher charge states of several protein ions can be formed than had been reported by use of *m*-NBA, sulfolane, and other supercharging additives. For example, by addition of 15% PC to solutions containing 44/54/1 methanol/water/acetic acid and 10 μM of cyt *c*, the average and highest observed charge states increased from 15.7 ± 0.1 and 21+ (no additive) to 21.9 ± 0.8 and 26+ (PC), which was significantly higher than by the use of 0.5% *m*-NBA (17.8 ± 0.2 and 24+) and 1% sulfolane (18.7 ± 0.4 and 24+).[29] EC can be used to shift nearly the entire CSDs of cyt *c* ions to higher charge states than the theoretical maximum limit that is based on proton transfer reactivity with the most basic solvent (methanol; 16+).[18a,29] Although relatively high concentrations of PC/EC were required to form "extremely" supercharged proteins,[29] these additives can be useful for narrowing CSDs.

Here, we report that 1,2-butylene carbonate (BC) and 4-vinyl-1,3-dioxolan-2-one (4V) can be added to ESI solutions at relatively low concentrations [5%(v/v)] to form protein ions in significantly higher charge states than by use of PC. The role of different additives (8 supercharging molecules, 12 acid molecules and 4 solvent molecules) on protein ion CSDs formed in ESI-MS was investigated. The extent of protein supercharging in ESI was strongly dependent on the strength the acid (*i.e.*, CSDs can shift by nearly 10 protons by using different acids), indicating that the extent of protein supercharging in ESI can be significantly limited by the binding of anions during ESI.

Methods

For ESI-MS experiments, a linear quadrupole ion trap MS (LTQ-MS; Thermo Scientific) was used. ESI solutions were infused into the ESI source (3 μl min^{-1}) and ions were formed by applying a voltage of +3 to 4.5 kV to the ESI capillary relative to the capillary MS inlet (250–450 °C; Table S1†). ESI solutions contained 5 μM protein, 5%(v/v) supercharger, 0.5% acetic acid and 94.5% distilled water (18 MΩ Milli-Q water), unless stated otherwise. All proteins, acids, supercharging additives, and organic solvents were obtained from commercial sources (electronic supplementary information†). For ECD and high-resolution MS, a hybrid LTQ-MS and 7 T Fourier transform ion cyclotron resonance MS (LTQ-FT/ICR-MS; Thermo Scientific) was used. Charge states were mass selected in the LTQ-MS (±5 *m*/*z* isolation window), thermalized by collisions with He(g) buffer gas (~1 mTorr),[30] and transferred to the FT-ICR for ECD (25 ms irradiation time; 3 eV initial energy). The automatic gain control was used to ensure that the ion trap was not overloaded (10 ms maximum ion accumulation time). ESI mass spectra were collected in triplicate and the uncertainty values were approximated by the standard deviation of these replicates (±1 standard deviation). Details of (i) circular dichroism, pH, and surface tension measurements; and (ii) the CD spectral analysis, and methods for calculating the average charge states (<*z*>), CSD widths (W_z; full-width at half max), electron capture efficiencies, fragmentation efficiencies, and sequence coverage are given in the electronic supplementary information.†

Results and discussion

Additive performance

Representative ESI mass spectra of aqueous solutions containing 5 μM cyt *c*, 0.5% acetic acid, and either no additional additive or one of seven different solution additives (BC, 4V, PC, 1,4-butanesultone, sulfolane, *m*-NBA, and 1,3-propanesultone) at "optimal" concentrations for maximising protein charging are shown in Fig. 1. The most abundant, the highest observed, and the average charge states of cyt *c* ions formed by use of each additive (*i.e.*, performance characteristics of supercharging) are shown in Table 1. By addition of any of these seven reagents, the CSD of cyt *c* ions increased from an average charge state of 14.7 ± 0.1 (no additive) to values that range from 16.5 ± 0.1 (1,3-propanesultone) to 22.6 ± 0.1 (4-vinyl-1,3-dioxolan-2-one). By addition of 5%(v/v) BC (or 4V), significantly higher charge states were formed than by use of the more traditional supercharging additives, PC,[29] sulfolane,[22a] and *m*-NBA[22c] under these conditions (Table 1). For example, by addition of BC, the average and maximum charge states were a respective 22.6 ± 0.2 and 26+, which was higher than the corresponding values for PC (21.8 ± 0.2, 25+), sulfolane (19.4 ± 0.3, 23+), and *m*-NBA (17.4 ± 0.2, 22+; 3% is near the solubility limit in acidified water).

For myoglobin, which is more acidic (pI *ca.* 7) than cyt *c* (pI *ca.* 10 to 11),[31] addition of 5% BC increased the average and highest observed charge states of protonated myoglobin from 20.6 ± 0.5 and 28+ (no additive) to 30.7 ± 0.1 and 34+ (Table 1); *i.e.*, a 50% increase in the average charge states (~10.1 protons). In contrast, the extent of myoglobin charging was lower by use of PC (29.8 ± 0.3 and 32+), sulfolane (26.1 ± 0.1 and 30+), and *m*-NBA (24.7 ± 0.6 and 30+). That is, BC (and 4V) can be used to form the highest known protonation states of cytochrome *c* and myoglobin (to our knowledge).

Effects of superchargers on CSDs

Based on these results, the relative order of supercharger effectiveness was (Table 1):

$$\text{BC} \approx \text{4V} > \text{PC} > \text{EC} > \text{1,4-butanesultone} > \text{sulfolane} > \textit{m}\text{-NBA} > \text{1,3-propanesultone}$$

Interestingly, as the effectiveness of protein superchargers increased, the width of the protein CSDs tended to narrow (Table 1). For example, the W_z values of the CSDs of myoglobin steadily decreased from 5.9 ± 1.7 to 1.7 ± 0.2 as the extent of charging increased from <*z*> = 20.9 ± 0.2 (1,3-propanesultone) to <*z*> = 30.6 ± 0.2 (4V). The origin of the CSD narrowing is not well understood. This effect might result from the presence of supercharging additives: (i) reducing the extent that protonation sites are neutralized by anion binding within droplets near the moment of ion formation, (ii) resulting in the for-

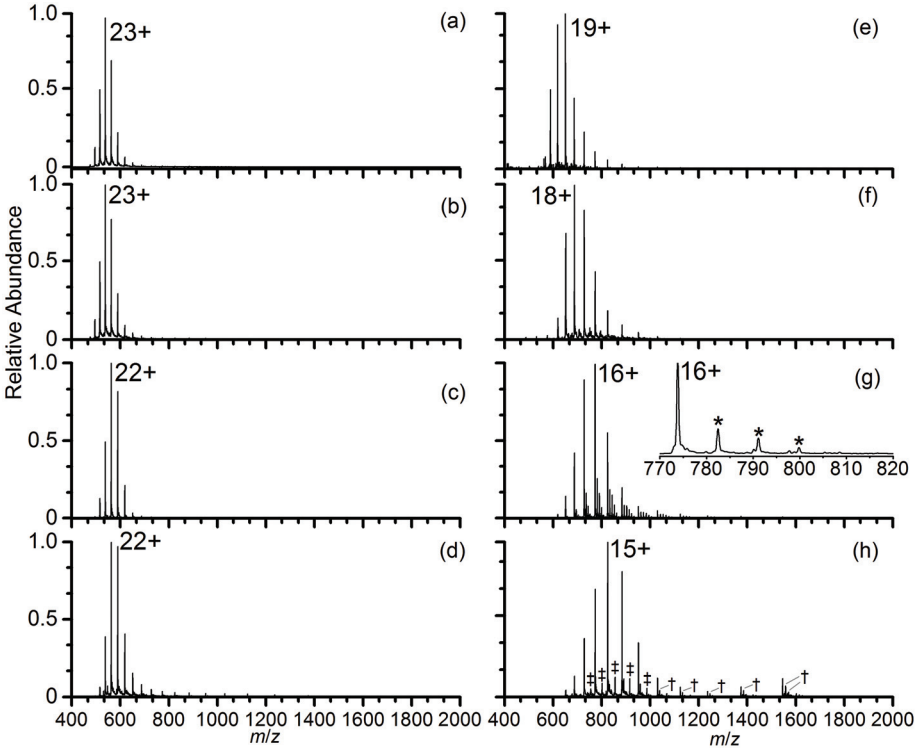

Fig. 1 Representative electrospray ionization mass spectra of aqueous solutions containing 5 μM cyt *c*, 0.5% (v/v) acetic acid, and (a) 5% 1,2-butylene carbonate, (b) 5% 4-vinyl-1,3-dioxolan-2-one, (c) 30% propylene carbonate, (d) 5% 1,4-butane sultone, (e) 3% sulfolane, (f) 3% *m*-NBA, (g) 5% 1,3-propane sultone, and (h) no supercharging additive. An ion series corresponding to [cyt *c*, *z*H, *n*(1,3-propane sultone)]$^{z+}$ is denoted by "*". Adducts correspond to +98 Da (phosphate) are denoted by "†" and chemical noise (12 810 Da; 17+ to 13+) is denoted by "‡".

Table 1 Performance characteristics of solution additives for increasing the extent of cytochrome *c* and myoglobin charging in ESI-MS

	Cytochrome *c*			Myoglobin		
SC[a]	z_{HOCS}/z_{MACS}[b]	<*z*>[c]	W_z[d]	z_{HOCS}/z_{MACS}	<*z*>	W_z
BC	26/23	22.6(0.2)	1.6(0.2)	34/31	30.6(0.2)	1.7(0.2)
4V	26/23	22.6(0.1)	1.3(0.1)	34/31	30.7(0.1)	1.9(0.1)
PC	25/22	21.8(0.2)	1.4(0.2)	32/30	29.8(0.3)	2.3(0.7)
EC	24/22	21.5(0.2)	2.6(0.1)	—	—	—
BuS	24/22	21.2(0.1)	2.1(0.3)	32/30	29.7(0.4)	3.6(0.9)
Sulf.	23/19	19.4(0.3)	2.9(3.5)	30/28	26.1(0.1)	3.4(0.5)
m-NBA	22/18	17.4(0.2)	3.8(2.0)	30/26	24.7(0.6)	4.9(0.8)
PS	22/16	16.5(0.1)	2.9(2.4)	28/22	20.9(0.2)	5.9(1.7)
None	20/15	14.7(0.1)	2.8(1.9)	28/21	20.6(0.5)	6.4(1.3)

[a] 5 μM protein in aqueous solutions containing 0.5% acetic acid. Optimal SC concentrations, %(v/v): 5% BC, 4V, 1,4-butanesultone (BuS), and 1,3-propanesultone (PS); 30% PC; 10% EC; 3% Sulf. and *m*-NBA. [b] z_{HOCS}/z_{MACS} are the highest observed charge state and the most abundant charge states. [c] Average charge state (standard deviation) of three replicate measurements. [d] Full-width-at-half maximum of Gaussian distributions that are fit to the observed charge state distributions (standard deviation values in parentheses).

mation mature ESI droplets that are more homogeneous with respect to size and composition, (iii) resulting in more homogenous conformational distributions of proteins near the moment of ion formation. The difference in the rate of proton transfer to residual solvent molecules between adjacent charge states may be significantly larger at very high charge densities than at lower charge densities, which could also contribute to CSD narrowing.[8a,32]

BC, 4V, 1,4-butanesultone and 1,3-propanesultone, which have not been used as ESI additives previously, were selected because they are chemical derivatives of known SCs and because these additives have relatively high surface tension values (>35 mN m^{-1}) and/or dipole moment values (*i.e.*, properties that are implicated in enhancing analyte charging in ESI; Table S2†).[9a,23] Although the extent of protein ion charging (Table 1) from these solutions does not strongly correlate

with surface tension and/or dipole moment values for this limited set of SC additives, the surface tension and dipole moment values are relatively high and should be comparable to the surface tension of water that contains a significant fraction of acetic acid, which is less volatile than water. For example, the surface tension of aqueous solutions containing acetic acid decrease from 51.4 to 41.2 mN m^{-1} as the acetic acid concentrations increase from 10 to 30% (m/m).[33] These surface tension values are lower than aqueous mixtures composed of 50% (62.5 mN m^{-1}) to 90% sulfolane (50.9 mN m^{-1}), which is significantly less volatile than water.[33] Because protein ion charging depends on a number of factors and the precise compositions of the droplets at the moment of ion formation are not well defined, identifying the primary effects that are responsible for increasing analyte supercharging in ESI is challenging.

Effects of acid identity

Representative mass spectra of aqueous solutions containing 5 μM cyt *c*, 5% 4V, and 0.5% of either acetic, iodic, nitric, or hydroiodic, or no acid are show in Fig. 2. Surprisingly, the identity of the acid has a dramatic effect on the extent of protein charging and the extent of acid adduction in ESI (*i.e.*, formation of [cyt *c*, *n*HA, *z*H]$^{z+}$). For example, by use of CH_3COOH and HIO_3 (weak acids), relatively high protein charge densities are obtained ($\langle z \rangle$ = 22.7 ± 0.4 and 20.6 ± 0.2, respectively) and the vast majority of the protein ion signal is assigned to [cyt *c*, *z*H$^+$]$^{z+}$ (>90%); that is, acid adduction is minimal and analyte charging is relatively high. In contrast, by use of HNO_3 or HI (strong acids), the average charge states are nearly ten protons lower than by use of the weak acids and the vast majority of the protein ion signal (>65%) is assigned to acid adducted protonated cyt *c*, [cyt *c*, *n*HA, *z*H]$^{z+}$ ($n \geq 1$). Moreover, the extent of charging with the strong acids ($\langle z \rangle$ = 14.8 ± 0.3 and 14.2 ± 0.2 for HNO_3 and HI acid, respectively) is only slightly higher than that obtained by not including any acid at all ($\langle z \rangle$ = 12.9 ± 0.5; Fig. 2e). The use of the strong acids results in broader CSDs (W_z = 2.7 ± 0.1 and 2.5 ± 0.1 for HNO_3 and HI acids) than by use of the weak acids (W_z = 1.3 ± 0.2 and 1.5 ± 0.1 for HIO_3 and acetic acid).

The average charge states of [cyt *c*, *z*H]$^{z+}$ that were formed upon ESI of solutions containing 5 μM cyt *c*, 0.5% of acid (HA = HI, $HClO_4$, HCl, H_2SO_4, HNO_3, HIO_3, $H_2C_2O_4$, H_3PO_4, HCOOH, C_6H_5COOH, CH_3COOH, and C_6H_5OH), and either no other additive or 5% of a supercharger (4V, 1,4-butanesultone, sulfolane, and 1,3-propanesultone) are plotted as a function of acid pK_a in Fig. 3. Significantly higher charge states were formed by use of any of the 7 weak acids (pK_a > 0) than by use of any of the 5 strong acids (pK_a < 0) for each of the four superchargers that were investigated (Fig. 3b–e). For example, by addition of 1,3-propanesultone, the average charge states of cyt *c* were between 16.5 and 14.5 for any of the of seven weak acids. For the strong acids, these values were between 13.2 and 12.4, which were nearly the same as that for the control solution that did not include any supercharging additive ($\langle z \rangle$ = 13.1 ± 0.1). For the more effective SCs, the average charge states of cyt *c* increased by an average of 8.6 (4V), 7.5 (sulfolane), and 7.1 (1,4-butanesultone) by using any of the 7 weak acids compared to any of the 5 strong acids. That is, the effectiveness of different SCs for enhancing analyte charging in ESI is significantly higher by use of weak acids than strong acids.

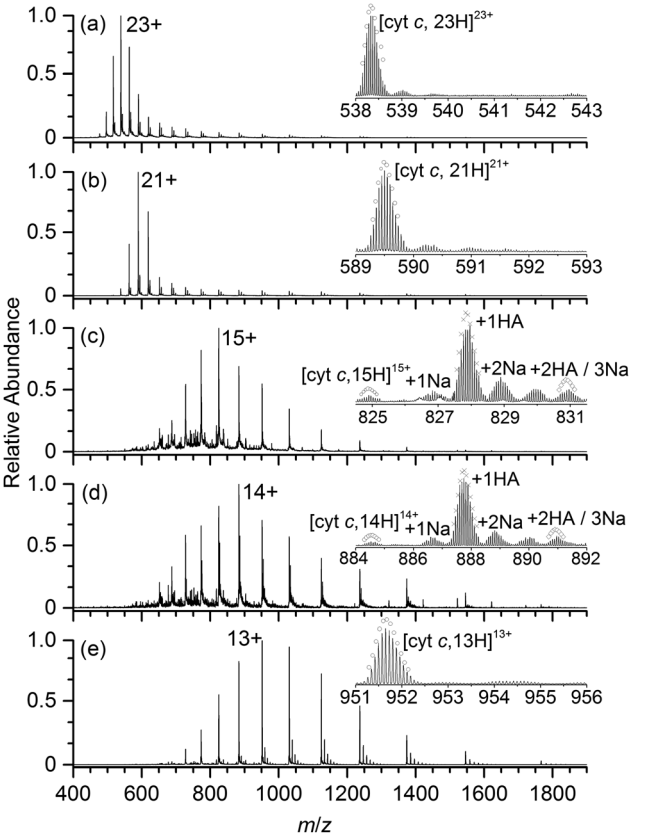

Fig. 2 ESI LTQ mass spectra of aqueous solutions containing 5 μM cyt *c*, 5% 4V, and 0.5% of either (a) acetic acid, (b) iodic acid, (c) nitric acid, (d) hydroiodic acid, or (e) no acid. Insets are FT-ICR mass spectra of the most abundant protein ion charge states. Theoretical isotope distributions for [cyt *c*, *z*H]$^{z+}$ (open circles) and [cyt *c*, *n*HA, *z*H]$^{z+}$ (crosses; denoted by +*n*HA) are shown. Ions assigned to [cyt *c*, *n*Na, (*z* − *n*)H]$^{(z-n)+}$ are denoted by +*n*Na. For panel (e), an ion series corresponding to [cyt *c*, *z*H, *n*4V]$^{z+}$ at <25% the most abundant ion [cyt *c*, 13H]$^{13+}$ was observed.

The extent of acid adduction (*i.e.*, relative formation of [cyt *c*, HA, *z*H]$^{z+}$ *vs.* [cyt *c*, *z*H]$^{z+}$) is significantly higher for cyt *c* ions formed from solutions that contain strong acids than those that contain weak acids (Fig. 3h–k). For example, by use of 0.5% of any of the 5 strong acids and 5% of 1,3-propanesultone, the relative formation of [cyt *c*, HA, *z*H]$^{z+}$ is between 57 and 77% (an average of 68.6 ± 7.8%). In contrast, by use of any of the 7 weak acids, the extent of acid adduction is ≤30%. Adduction of strong acids *vs.* weak acids is also dramatically higher for cyt *c* ions formed from solutions that contain the other three more effective supercharging additives (Fig. 3h–j); *i.e.*, this effect is relatively general. Acid adduction can decrease with increasing analyte charge density owing to the increased energy deposited into more highly charged ions

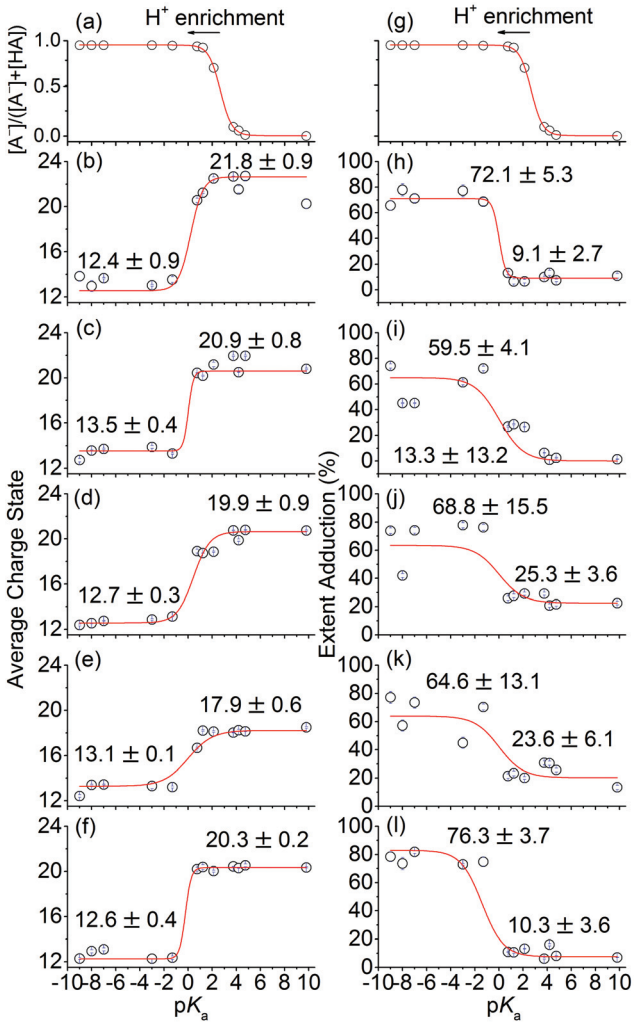

Fig. 3 The fraction of acid molecules that were ionized (HA → $H^+ + A^-$) in solution prior to ESI (a, g). The average charge states of $[\text{cyt } c, z\text{H}]^{z+}$ (b–e) and extent of acid (HA) adduction (*i.e.*, $[\text{cyt } c, n\text{HA}, z\text{H}]^{z+}$; h–k) that were obtained from ESI mass spectra of aqueous solutions containing 5 uM cyt *c*, 0.5% acid (HI, $HClO_4$, HCl, H_2SO_4, HNO_3, HIO_3, $H_2C_2O_4$, H_3PO_4, HCOOH, C_6H_5COOH, CH_3COOH, C_6H_5OH), and (b, h) 5% 4V, (c, i) 5% 1,4-butanesultone, (d, j) 5% sulfolane, and (e, k) 5% 1,3-propanesultone *vs.* the pK_a value of the acid. (f, l) The average charge states and extent of acid adduction obtained by use of 5% 4V in 1 : 1 water : methanol with 0.5% acid *vs.* acid pK_a values (*i.e.*, control data for ion conformation effects). For each supercharger, all ESI-MS instrument parameters were kept constant. The average ordinate values of 7 weak acids and 5 strong acids are given.

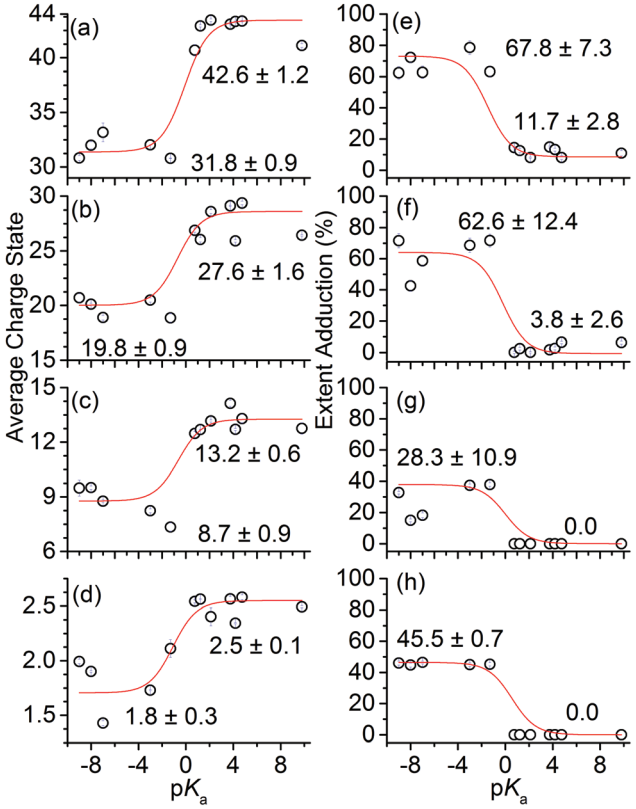

Fig. 4 The average charge states (a–d) and extent of acid (HA) adduction (e–h) that were obtained from ESI mass spectra of aqueous solutions containing 5% 4V, 0.5% acid (same acids as Fig. 3), and (a, e) 5 μM CAII, (b, f) 5 μM myoglobin, (c, g) 5 μM ubiquitin, (d, h) 5 μM AII *vs.* the pK_a of the acid. For each analyte, all ESI-MS instrument parameters were kept constant. The average ordinate values of 7 weak acids and 5 strong acids are given.

than lower charged ions, which should result in the loss of neutral HA molecules.[16]

Effects of acid concentration

The average charge states, CSD widths, and extent of acid adduction of protonated cytochrome *c* as a function of acid concentration for aqueous solutions containing 5 μM cytochrome *c*, 5% BC and between 0.5% to 5% of either acetic acid (weak acid) or hydrochloric acid (strong acid; 0.5 to 2.5%) are shown in Table S3.† As the concentration of acetic acid increased from 0.5 to 5%, the average charge state of protonated cytochrome *c* monotonically decreased from 22.6 ± 0.2 to 16.6 ± 0.1, the CSDs broadened from W_z values of 1.6 ± 0.2 to 3.5 ± 0.8, and the extent of acid adduction increased from 7.3 ± 1.0 to 38.9 ± 5.1% (Table S3†). For HCl, as the acid concentration increased from 0.5% to 2.5%, the average charge states decreased monotonically from 13.6 ± 0.1 to 11.8 ± 0.1, the widths of the CSDs broadened from W_z values of 2.7 ± 0.1 to 4.2 ± 0.7, and the extent of acid adduction slightly increased or stayed the same from 71.2 ± 3.2 to 87.6 ± 10.3 (Table S3†); *i.e.*, significantly higher analyte charge densities were formed by use of the weak acid (acetic acid) than the strong acid (HCl), including by use of acetic acid concentrations [%(v/v)] that were a factor of 5 higher (or lower) than that of HCl under these conditions. These results indicate that the strong dependence of protein supercharging by use of strong compared to weak acids (Fig. 3 and 4) does not result from differences in the initial molar concentrations of the acids. Because the extent of charging decreases, the extent of acid adduction increases, and the charge states broaden as the concentration of HCl and acetic acid increases, these data are consistent with the neutralization of protein protonation sites by the binding

of conjugate base anions of the acids limiting the extent of protein supercharging in ESI.

Other correlations?

Recently, the extent of protonated protein ion charging by use of nitrophenol and sulfolane was reported to be limited by ion-paring (*i.e.*, the formation of anion adduction to protonated analytes),[26] which was rationalized by using the best-match gas-phase basicity model for positively charged analytes in relatively low charge states that are relatively basic.[34] In this model, R-NH_2···H^+···A^- interactions (where R-NH_2 is a basic site and A^- is an anion) will be most favourable if the apparent GB of the amine is close to the GB of the anion.[34] In our experiments, similar extents of acid adduction were observed by use of perchloric acid [GB(A^-) = 1200 kJ mol^{-1}; strong acid] and HCl [GB(Cl^-) = 1374 kJ mol^{-1}; strong acid].[35] However, the GB values differ by 174 kJ mol^{-1} (Fig. S1†). Moreover, the GB of Cl^- is 23 and 51 kJ mol^{-1} *higher* than those for $H_2PO_4^-$ and $HC_2O_4^-$,[35] respectively, and the extent of acid adduction values by use of H_3PO_4 and $H_2C_2O_4$ (weak acids) were significantly lower than that for HCl. That is, the extent of protein ion charging did not correlate with the GB values of the anions (Fig. S1†). The GB values of the 12 conjugate base anions ion our experiments range from 1200 kJ mol^{-1} (ClO_4^-) to 1432 kJ mol^{-1} (deprotonated phenol). Williams and co-workers have measured the apparent GB of protonated cytochrome *c* ions,[18b] which decreased from 980 kJ mol^{-1} (3+) to 801 kJ mol^{-1} (15+) as charge states increased; *i.e.*, the GB^{app} values of protonated cytochrome *c* ions are more than 200 kJ mol^{-1} lower than the GB of the least basic anion of the 12 acids investigated. The difference between the GB of the anions and the GB^{app} of the protein ions should continue to increase as the charge states increase because Coulomb repulsion will increase and the number of basic sites that are available for protonation will decrease as charge states increase. Given the large difference in GB and GB^{app} values between the 12 anions and extensively protonated protein ions (>200 kJ mol^{-1}), it is not expected that the GB of the anions should necessarily correlate with the extent of protein ion charging and acid adduction based on the matching GB model for protonated protein ions in relatively low charge states. In addition, the extent of cyt *c* charging as a function of acid identity (Fig. 3) did not strongly correlate with (i) the proton affinity (PA) values of the conjugate base anions of the acids (A^-); and (ii) the GB/PA of the neutral acids (Fig. S1†).

The relative difference in the extent of protein ion charging (and extent of acid adduction) by use of strong acids compared to weak acids did not correlate with acid volatility (*e.g.*, Henry's Law constants, boiling points, and/or vapour pressures; Fig. S2 and Table S4†). For example, the boiling point and Henry's law constant for HCl (strong acid) are −85 °C and 1.5×10^1 mol m^{-3} Pa^{-1} and those for benzoic acid are 249 °C and 2.9×10^2 mol m^{-3} Pa^{-1}, respectively. The average charge states and extent of acid adduction for cytochrome *c* by use of benzoic acid is 21.5 ± 0.3 and 13.2 ± 1.9%, whereas that for HCl is 13.6 ± 0.1 and 71.2 ± 3.2%. These data suggest that the acids do not necessarily need to be non-volatile (or volatile) to effectively quench protein supercharging.

In solution, different anions can destabilize protein structure to different extents (*i.e.*, Hofmeister effects).[36] Williams and co-workers determined that the extent of "electrothermal" supercharging of proteins from native solutions (increasing protein charging by increasing the electric field between the ESI capillary and the capillary entrance to the mass spectrometer) that contained ammonium salts of a range of Hofmeister anions strongly correlated with a reverse Hofmeister series.[36a] In our experiments, the extent of charging does not correlate with the Hofmeister series (Fig. S3†). The proteins should be largely denatured prior to ESI (see below) and thus, protein structural effects are not expected to significantly affect the extent of analyte charging in ESI. Collectively, these data were most consistent with acid strength strongly affecting the extent of protein supercharging in ESI when compared to GB and PA values (of HA and A^-), the relative volatility of the acids, and/or the relative extent that A^- can destabilize protein structures (Hofmeister effects) under these conditions.

Effects of analyte size

The effects of acid identity were investigated for carbonic anhydrase II (CAII) (29 kDa), myoglobin (17 kDa), ubiquitin (8.6 kDa), and angiotensin II (AII; 1032 Da), the latter of which should essentially eliminate any tertiary structural effects (Fig. 4). For each analyte, significantly higher analyte charge densities (and significantly less acid adduction) are formed by use of weak acids than strong acids. For example, addition of any of the 7 weak acids to solutions containing 4V results in average charges of $[CAII, zH]^{z+}$ that range from between 43.4 and 40.7 (and average acid adduction of 8.1 to 15.8%), which are an average of 10.8 protons higher than the average charge states obtained for each of the 5 strong acids (average adduction of 62.7 and 77.6%). By use of weak acids, an average of 7.8, 4.4 and 0.7 more protons ionize myoglobin, ubiquitin and AII than by use of strong acids. These results indicate that the pK_a switch at a value of *ca.* 0 between the formation of relatively high analyte charge densities (and low acid adduction) *vs.* low charge densities (and high acid adduction) is a relatively general phenomenon for a reasonably broad range of analyte sizes (1 to 29 kDa).

For ESI solutions that did not contain SCs, the extent of analyte charging did not depend as strongly on the identity of the acid as those formed from solutions that contained supercharging additives for CAII, myoglobin, ubiquitin, and AII and the 12 different acids (Fig. S4†). However, the extent of acid adduction was significantly higher by use of strong acids than weak acids (Fig. S4†). These data indicate that the switch in the extent of acid adduction that occurs at pK_a values of *ca.* 0 also occurs for solutions that do not contain SCs (Fig. S4†) in addition to those that contain SCs (Fig. 3 and 4). In general, the difference in the extent of charging by use of strong compared to weak acids monotonically increased with as the effectiveness of the solution for enhancing protein ion charging increased. The relatively minor dependence of the extent of

protein ion charging on acid strength in ESI (no SC additive; Fig. S4†) can result from the preferential enrichment of conjugate base anions of strong acids compared to those for weak acids; *i.e.*, the neutralization of protein ion charge sites by anion binding can counteract the effect of lower solution pH values (and higher anion concentrations) on the extent of protein ion charging in ESI (with or without SC additives). During the ESI process, the conjugate base anions of strong acids should be enriched to a greater extent than weak acids to the extent that the proton concentration is not sufficiently high to neutralize a significant fraction of the anions of strong acids on the timescale of droplet evaporation, fission, and ion formation (droplet lifetimes of ms to sub-ms).[12a,37]

Effects of gaseous ion conformation(s)

Protonated cytochrome *c* ions were formed in charge states that ranged from 10 to 25+ depending on the identity of the acid and supercharger (Fig. 3), which corresponds to between 1.0 and 2.4 charge sites per 10 amino acid residues. For ubiquitin, values of between 1 and 3 charges per 10 amino acid residues were formed under these conditions (Fig. 4). By use of ion-mobility mass spectrometry, Clemmer and co-workers measured the collisional cross sections of protonated ubiquitin and cytochrome *c* ions that were formed by ESI as a function of charge state.[5a,b] For ubiquitin and cytochrome *c* ions, compact and partially folded protein ion structures were formed for the *ca.* 4 to 9+ charge states.[5a,b] For 10+ and higher charge states, elongated structures were formed. That is, elongated protein ion structures can be formed for protonated protein ions that have an average of *ca.* 1 or more charges per 10 amino acid residues. These data suggest that in our experiments, the protein ions should be elongated and any gas-phase tertiary structural effects on the extent of protein ion charging[5c] should be minimal.

For solutions that contain a large fraction of organic protein denaturing solvent (50% methanol), the use of strong acids also quenches protein supercharging and results in relatively high acid adduction, whereas the use of weak acids results in the formation of protein ion charge states with more charge and less acid adduction (Fig. 3). For a small peptide (angiotensin II; 1.0 kDa) that should have minimal tertiary structure, the use of strong acids also resulted is less analyte charging and more acid adduction than by the use of weak acids (Fig. 4). Collectively, these results indicate that the strong dependence of protein ion charging and acid adduction on the acid strength is not a result of tertiary gaseous ion conformational effects under these conditions.

Effects of acids on CSD widths

For the supercharged proteins/peptide ions (cyt *c*, CAII, myoglobin, ubiquitin), the widths of protein CSDs are relatively narrow for the weak acids and are relatively broad for the strong acids (Fig. S5 and S6†). For example, the widths of the protonated CAII CSDs formed from aqueous solutions containing 5 μM CAII, 5% 4V, and 0.5% acid are significantly higher for the 7 weak acids (the average W_z value for all 7 weak acids is 2.3 ± 0.8) than that for the 5 strong acids (average W_z value for all 5 strong acids is 5.2 ± 0.9). For the other proteins, the CSDs that are formed from solutions containing weak acids are also broader than those containing strong acids. For example, the average W_z values for all strong acids were a respective 2.7 ± 0.1, 4.6 ± 0.3, and 1.6 ± 0.2 for cyt *c*, myoglobin and ubiquitin, which are broader than the corresponding values for the 7 weak acids (1.6 ± 0.2, 2.7 ± 0.4, and 0.8 ± 0.1, respectively); that is, the use of weak acids narrows the protein ion CSDs by between 40% to 70%. The CSDs were also wider for the strong acids *vs.* weak acids for aqueous solutions containing different SCs (Fig. S4†). For example, ESI-MS of 5 μM cyt *c*, 0.5% acid (any of the 12 different acids), and 5% of either 1,4-butanesultone, sulfolane, or 1,3-propanesultone resulted in an average W_z value for all 5 strong acids of 2.8 ± 0.1, 2.7 ± 0.4, and 3.7 ± 0.9 *vs.* the corresponding values of 2.1 ± 0.6, 1.7 ± 0.2, and 2.0 ± 0.4 for the 7 weak acids; that is, an average CSD narrowing of 25% to 46% by use of weak acids compared to strong acids. These data indicate that the binding of conjugate base anions of acids to protonated protein ions can result in broader protein CSDs and less analyte charging.

Effects of additives on protein structures in solution

Circular dichroism (CD) spectra were obtained for aqueous solutions that contained 50 μM cyt *c* with 0.5% acid (or no acid) and between 0 and 9% 4V (Fig. 5). For concentrations

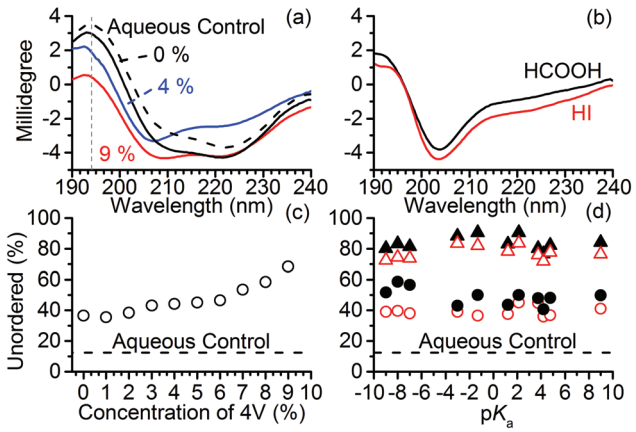

Fig. 5 (a) Circular dichroism (CD) spectra of 50 μM cyt *c* in aqueous solutions containing 0.5% acetic acid and either 0 (solid black curve), 4 (solid blue curve), or 9% 4V (solid red curve). The CD spectra of the aqueous control (dashed black trace), contains 50 μM cyt *c* (no acid; no supercharging additive). More negative values at 194 nm (grey dashed line) are generally indicative of less ordered protein structure.[38] (b) CD spectra of 50 μM cyt *c* in an aqueous solution that contains 0.5% of either a strong (HI) or weak acid (HCOOH) and no supercharging additive. (c) Relative extent that cyt *c* (50 μM) is unordered in aqueous solutions that contain 0.5% acetic acid and between 0 and 9% 4V *vs.* the concentration of 4V. (d) Relative extent that cyt *c* (50 μM) is unordered in aqueous solutions containing: (i) 0.5% of acid (same acids as in Fig. 2); (ii) either no supercharging additive (open red circles) or 5% 4V (solid black circles); and (iii) in 1 : 1 water : methanol containing 0.5% of acid and either no supercharging additive (open red triangles) or 5% 4V (solid black triangles) *vs.* acid pK_a values.

>9%(v/v), 4V saturated the solution. Generally, the CD band at *ca.* 194 nm (assigned to the $\pi \rightarrow \pi^*$ transition of the peptide bond)[38] decreased to less positive values, as the concentration of 4V increased (Fig. 5a), which indicates that the relative extent of protein disorder increased as the concentration of 4V increased.[38] The CD deconvolution algorithm (CONTIN) can be used to approximate the relative extent that a protein is unordered by fitting the CD data (190 to 240 nm) with a linear combination of CD spectra from 16 standard proteins.[38] Addition of 0.5% (v/v) acetic acid (no 4V) increased the calculated extent of unordered cyt *c* from *ca.* 10% (aqueous control) to 36% (Fig. 5c). In general, the relative extent of unordered cyt *c* increased from 36% to 68% as the concentration of 4V increased from 0 to 9%(v/v), indicating that 4V can denature protein secondary structures in aqueous solutions. These results (Fig. 3 and 5) are consistent with the hypothesis that enrichment of supercharging additives during the ESI process can chemically denature protein structures and result in more elongated protein ion conformations that can accommodate higher charge states when formed from "native" ESI solutions.[22b,39]

CD spectra of cyt *c* in aqueous solutions and 1 : 1 water : methanol that contain 0.5% of each of the 12 acids were obtained. For both the acidified aqueous and the 1 : 1 methanol : water solutions, the CD spectra do not correlate with acid strength for all 12 acids. For example, the CD spectra for HCOOH (pK_a = 3.75) and HI (pK_a = −9) are very similar (48.2 and 50.6% unordered, respectively; Fig. 5b). The average calculated extent of unordered protein that is obtained for all 12 acids increases from 49.1 ± 5.5% (with 4V) and 39.5 ± 4.5% (no 4V) for the aqueous solutions to 83.6 ± 4.4% (with 4V) and 77.3 ± 4.2% (no 4V) for the 1 : 1 methanol : water solutions, which is consistent with the addition of methanol denaturing protein secondary structures. Overall, these results indicate that the strong dependence of protein supercharging in ESI on the use of strong compared to weak acids (Fig. 3 and 4) does not result from (i) differences in the solution-phase protein structure(s) in solution prior to ESI from either acidified aqueous solutions or acidified methanol : water solutions and/or (ii) differences in protein denaturation as the composition of the droplets change owing to preferential evaporation; *i.e.*, the strong dependence of protein ion supercharging on acid strength does not result from changes in protein ion conformation in solution, the gas-phase, and during desolvation by use of the different acids.

Mechanism and "effective" pH of ESI droplets

In our experiments, the initial ESI solutions prior to ESI contain a significant fraction of water and the pH of the solutions that contain strong acids are between 1.0 and 1.2 ± 0.1 pH units (*i.e.*, >99% ionized), while those containing weak acids are between 2.6 ± 0.1 and 3.1 ± 0.1 pH units (Table 2). The measured pH values do not significantly change by use of 5%(v/v) 4V (Table 2). From the pH measurements of the ESI solutions prior to ESI and the Henderson–Hasselbalch equation, the fraction that each acid is ionized prior to ESI can be obtained (Fig. 3a). For the weak acids with pK_a values that were lower than the pH of the respective solutions, the extent that the acid molecules were ionized prior to ESI were 98%, 97%, and 75% for HIO_3, $H_2C_2O_4$ and H_3PO_4, respectively (Fig. 3a). For the weak acids with pK_a values greater than the pH of the respective solutions (HCOOH, C_6H_5COOH, CH_3COOH, C_6H_5OH), the extent the acids were ionization prior to ESI were <10% (Fig. 3a). For ESI, ionic droplets are preferentially enriched with less volatile solution components (*i.e.*, ions and supercharging additives)[22b,27] and the relative concentrations of these components should not be at equilibrium owing to rapid desolvation and droplet fissioning events. For positively charged droplets formed from acidified solutions, enrichment of H_3O^+ ions during desolvation can lower the pH.

Table 2 pH values of aqueous solutions containing 0.5% acid (Soln. A), 0.5% acid and 5% 4V (Soln. B), and 0.5% acid, 5% 4V, and 5 μM cytochrome *c* (Soln. C)[a]

Acid	Soln. A	Soln. B	Soln. C
HI	1.1	1.1	1.1
$HClO_4$	1.2	1.2	1.2
HCl	1.0	1.0	1.0
H_2SO_4	1.1	1.1	1.1
HNO_3	1.1	1.0	1.0
Iodic	2.6	2.6	2.6
Oxalic	2.8	2.8	2.8
H_3PO_4	2.7	2.6	2.6
Formic	2.7	2.8	2.8
Benzoic	3.1	3.0	3.0
Acetic	2.9	2.8	2.8
Phenol	3.0	3.1	3.1
No Acid	7.0	7.0	7.0

[a] The standard deviation of three replicate measurements were <0.1 pH units.

Because the extent of protein supercharging is significantly higher, acid adduction is significantly lower, and the CSDs are narrower by use of many different weak acids *vs.* strong acids (for many different sizes of proteins/peptides) and because these data do not correlate with proton affinity, gas-phase basicity, and/or protein conformation (see above), these results suggest that the charging and supercharging of protein ions in ESI can be significantly limited by the pairing of conjugate base anions and protonation sites in protein ions. Ion-pairing (*e.g.*, $R\text{-}NH_2\cdots H^+\cdots A^-$ interactions) could occur during ion formation or within the ESI generated droplets prior to the moment of ion formation. The resulting neutral acid molecules that are non-covalently bound to the protein ions can be readily lost,[16] which results in the overall loss of one charge from the protein ion per anion binding event. The anions of strong acids can be preferentially enriched in the droplets during ESI and the concentration of protons in the resulting droplets may not be sufficiently high to neutralize a significant fraction the strong acids on the timescale of ESI droplet desolvation and ion formation (ms to sub-ms)[12a,37] to significantly reduce the extent of ion-pairing (Fig. 3). In contrast, a smaller

fraction of the weak acid molecules should be ionized than that for the strong acids in the ESI droplets upon proton enrichment (Fig. 3a), which should reduce the extent that anions of weak acids neutralize protonation sites during the droplet desolvation and ion formation processes.

Overall, these data suggest that (i) the effective pH values of the droplets that are formed from solutions containing weak acids are sufficiently lower than the pK_a values of the acids to significantly reduce the neutralization of protonation sites on the timescale of droplet desolvation and ion formation; and (ii) the effective pH values of the droplets that are formed from solutions that contain strong acids are sufficiently higher than the pK_a of the acids to result in significant anion binding to protonated protein ions. The term "effective" is used to acknowledge that these values were inferred from experimental data for ionic droplets with compositions, sizes, and temperatures that are not well-defined and rapidly changing; *i.e.*, these values do not correspond to direct equilibrium measurements. The average and standard deviation of the 8 abscissa inflection points obtained from the best-fit sigmoid functions in Fig. 3 and 4 were −0.2 and 0.3, respectively. For the solutions that contain acids with pK_a values near 0 (nitric, oxalic and iodic acids), these data indicate that the effective pH values of the ESI generated droplets that result in the formation of detectable protein ions are near 0 (Fig. 3 and 4). The effective pH values obtained from the inflection points are not significantly affected by the identity (or presence) of SCs for at least 4 different additives that differ significantly in their effectiveness for supercharging analyte ions in ESI (Fig. 3). In addition, the inflection points are not shifted significantly by the use of 50% methanol (Fig. 3). SC additives and methanol may not strongly affect the preferential enrichment of the conjugate base anions of strong acids (>99% ionized prior to initiating ESI) during droplet desolvation when formed from solutions that contain a significant fraction of water under these conditions.

Gatlin and Turećek inferred that the pH of relatively neutral water/methanol solutions decrease by 3–4 pH units based on the dissociation of $M^{2+}(bpy)_3$, M = Fe and Ni, in ESI-MS and solution equilibria calculations.[14] By use of laser-induced fluorescence of a pH sensitive fluorescent probe molecule in ESI generated droplets, Cook and co-workers determined that the pH of ESI droplets can decrease by ≥1 pH unit when formed from near-neutral solutions.[13] The decrease in the pH of *ca.* 1 to 3 pH units that is inferred from our results (Fig. 3 and 4, Table 2) is consistent with these previous reports.

Effects of solvent

Mass spectra of $[\text{cyt } c, z\text{H}]^{z+}$ were obtained by ESI of solutions containing 5 μM cyt c, 5% 4V, 0.5% acetic acid, and 94.5% of either water (GB = 157.7 kcal mol^{-1}; γ = 71.99 mN m^{-1}), methanol (173.2 kcal mol^{-1}; 22.07 mN m^{-1}), acetonitrile (179.0 kcal mol^{-1}; 28.66 mN m^{-1}), or isopropanol (182.3 kcal mol^{-1}; 20.93 mN m^{-1}; Fig. S7†).[33,35] The extent of $[\text{cyt } c, z\text{H}]^{z+}$ charging followed this trend: water ($\langle z \rangle$ = 22.6 ± 0.2) > methanol (21.7 ± 0.3) ≈ acetonitrile (21.5 ± 0.4) > isopropanol (20.7 ± 0.3). For solutions that do not contain supercharging additives, the extent of protein ion charging for three proteins (myoglobin, cytochrome *c*, and ubiquitin) in ESI-MS by use of solutions that contain 5 μM of protein, 0.5% acetic acid, and no supercharging additive and 99.5% solvent (solvent = methanol, acetonitrile, and isopropyl alcohol) are shown in Fig. S8.† High organic solvent concentrations (>99%) were used to ensure that the mature ionic droplets that are formed from these solutions in ESI should contain a significant fraction of the organic solvent and that protein ion conformational effects should be minimal. The extent of cytochrome *c* charging by use of 99.5% methanol (15.1 ± 0.3), acetonitrile (14.8 ± 0.2) and isopropanol (14.2 ± 0.2) were the same or slightly decreased as the GB of the solvent increased and surface tension decreased. For ubiquitin (and myoglobin) and for solutions containing 50/50 water/solvent (solvent = methanol, acetonitrile, isopropyl alcohol; no supercharger), the same general trends were observed (Fig. S8†); *i.e.*, the extent of charging stayed the same or decreased slightly as the GB of the solvent increased and surface tension decreased. These data are consistent with results for protein ions that were formed from denaturing solutions that did not contain SCs.[8a] These data suggest that protein supercharging can be (i) limited by gas-phase proton transfer reactions with solvent molecules[8a] (in addition to the neutralization of protonation sites by anions within ESI generated droplets); and (ii) maximised by selecting water in preference to other common ESI solvents. These data are also consistent with the hypothesis by Williams and co-workers (for denatured protein ions) that higher droplet surface tension values can result in increased analyte charging.[9a]

Loo *et al.* have proposed that analyte charging can be enhanced by the use of ESI additives that have conjugate acids (*i.e.*, the protonated additive) that have pK_a values that are lower than that of water (<−1.7)[26] and are enriched to a significant extent during the ESI process owing to preferential evaporation. Methanol (pK_a = −2; vapour pressure = 127 mmHg), acetonitrile (pK_a = −10; 88.8 mmHg) and isopropyl alcohol (pK_a = −2.2; 45.4 mmHg)[40] all have significantly more negative pK_a values for the corresponding conjugate acids (SH^+) than protonated water (pK_a = −1.7) and these solvents are more volatile than water (23.8 mmHg). Given that (i) acetonitrile has a pK_a that is 5.0 and 4.5 times lower than methanol and isopropyl alcohol, respectively; (ii) the volatility of acetonitrile (88 mmHg) is between that of methanol (127 mmHg) and isopropyl alcohol (45.4 mmHg); and (iii) the extent of protein ion charging by use of 99.5% acetonitrile, methanol and isopropyl alcohol were nearly the same (Fig. S8†), these data are inconsistent with the hypothesis that the addition of additives that have low pK_a values (for the protonated neutral additives; SH^+) should necessarily enhance analyte charging.[26] That is, these data are more consistent with analyte charging being limited by gas-phase proton transfer reactivity[8a] and/or surface tension.[9a]

Improving ion dissociation

By use of ESI and BC, [ubiquitin, 17H]$^{17+}$ can be formed, readily isolated, and trapped in a 7 T FT-ICR MS (Fig. S9†). Electron capture by [ubiquitin, 17H]$^{17+}$ resulted in the formation of an extensive number of relatively non-specific cleavages along the backbone of the protein ion (*i.e.*, 223 cleavages identified; Fig. S10†) from which 74 of 75 possible unique inter-residue cleavage sites can be identified (99% sequence coverage). In contrast, ECD of [ubiquitin, 13H]$^{13+}$, which was the highest charge state that could be isolated without the use of SC additives, resulted in the identification of 109 cleavages and 44 of 75 inter-residue sites (59%). In addition, the ECD efficiency and fragmentation efficiency increased significantly from a respective 79% and 69% for [ubiquitin, 13H]$^{13+}$ to 97% and 92% for [ubiquitin, 17H]$^{17+}$. McLafferty and co-workers reported that by combining data for ECD and collisional activation dissociation from many charge states (7 to 13+) of ubiquitin, complete sequence can be assigned (seven charge states).[41] For electron transfer dissociation (ETD) of [ubiquitin, 10H]$^{10+}$, 65 out of 75 unique inter-residue cleavage sites were identified.[42] Here, the identification of 74 of 75 unique inter-residue cleavage sites corresponds to the highest sequence coverage that has been reported for a single isolated charge state of ubiquitin by ECD or ETD (to our knowledge).

Conclusions

1,2-Butylene carbonate and 4-vinyl-1,3-dioxolan-2-one can be added to ESI solutions in relatively low concentrations to effectively form protein ions in higher charge states than by use of other known additives and methods. Protein supercharging is significantly more effective by use of water than by use of organic solvents that have high GB values and are commonly used in ESI (*e.g.*, acetonitrile and methanol), indicating that these additives should be avoided to maximize analyte charging. Because these organic solvents are significantly less basic than water in bulk solution, acid/base proton transfer reactions with *neutral* solution additives in ESI generated droplets do not significantly limit analyte charging under these conditions. However, the anions of strong acids (pK_a values <0; >99% ionized prior to ESI) can effectively quench protein supercharging, broaden protein CSDs, and result in significant acid adduction to protein ions in ESI, whereas weak acids (pK_a values >0) result in high analyte charge densities, narrow CSDs, and minimal acid adduction, indicating that anion binding can dramatically reduce analyte charging and supercharging in ESI. From these data, the effective pH of ESI generated droplets formed from acidified aqueous protein-denaturing solutions near the moment of ion formation can be near 0, which was between 1 and 3 pH units lower than the solutions from which the ESI droplets were formed. As the effectiveness of supercharging increased for 8 different additives, the protein CSDs narrowed significantly. These results indicate that by discovering even more effective supercharging additives it should be possible to narrow protein ion CSDs further, which should prove beneficial for improving the performance of many MS and tandem-MS measurements. For example, by use of 1,2-butylene carbonate, ESI-MS, and ECD, 99% of all inter-residue amino acid sites can be identified from an ECD mass spectrum of a single isolated charge state of ubiquitin (223 total sequence ions; 92% fragmentation efficiency).

Acknowledgements

We thank Sydney Liu Lau and Associate Professor Mark Raftery (Bioanalytical MS Facility; BMSF) for helpful discussions. MAZ acknowledges the BMSF for an Honours Research Scholarship. WAD thanks the Australian Research Council for a Discovery Early Career Research Award fellowship.

References

1 (*a*) J. B. Fenn, M. Mann, C. K. Meng, S. F. Wong and C. M. Whitehouse, *Science*, 1989, **24**, 8; (*b*) N. B. Cech and C. G. Enke, *Mass Spectrom. Rev.*, 2001, **20**, 362; (*c*) P. Kebarle and U. H. Verkerk, *Mass Spectrom. Rev.*, 2009, **28**, 898.

2 (*a*) A. R. Dongré, *et al.*, *J. Am. Chem. Soc.*, 1996, **118**, 8365; (*b*) G. Tsaprailis, *et al.*, *J. Am. Chem. Soc.*, 1999, **121**, 5142; (*c*) B. A. Cerda, *et al.*, *J. Am. Soc. Mass Spectrom.*, 2001, **12**, 565; (*d*) G. E. Reid, *et al.*, *Anal. Chem.*, 2001, **73**, 3274; (*e*) B. Paizs and S. Suhai, *Mass Spectrom. Rev.*, 2005, **24**, 508; (*f*) T. G. Flick, W. A. Donald and E. R. Williams, *J. Am. Soc. Mass Spectrom.*, 2013, **24**, 193; (*g*) M. G. Leeming, *et al.*, *J. Am. Soc. Mass Spectrom.*, 2014, **25**, 427.

3 (*a*) R. A. Zubarev, *Curr. Opin. Biotechnol.*, 2004, **15**, 12; (*b*) H. J. Cooper, K. Hakansson and A. G. Marshall, *Mass Spectrom. Rev.*, 2005, **24**, 201; (*c*) R. A. Zubarev, N. L. Kelleher and F. W. McLafferty, *J. Am. Chem. Soc.*, 1998, **120**, 3265; (*d*) R. A. Zubarev, *et al.*, *Anal. Chem.*, 2000, **72**, 563; (*e*) D. M. Horn, Y. Ge and F. W. McLafferty, *Anal. Chem.*, 2000, **72**, 4778.

4 (*a*) R. A. Zubarev, *et al.*, *Eur. J. Mass Spectrom.*, 2002, **8**, 337; (*b*) W. A. Donald, *et al.*, *Proc. Natl. Acad. Sci. U. S. A.*, 2008, **105**, 18102; (*c*) W. A. Donald, *et al.*, *J. Am. Chem. Soc.*, 2010, **132**, 4633; (*d*) W. A. Donald and E. R. Williams, *J. Am. Soc. Mass Spectrom.*, 2010, **21**, 615; (*e*) W. A. Donald and E. R. Williams, *Pure Appl. Chem.*, 2011, **83**, 2129.

5 (*a*) K. B. Shelimov, *et al.*, *J. Am. Chem. Soc.*, 1997, **119**, 2240; (*b*) S. J. Valentine, A. E. Counterman and D. E. Clemmer, *J. Am. Soc. Mass Spectrom.*, 1997, **8**, 954; (*c*) L. Konermann and D. J. Douglas, *J. Am. Soc. Mass Spectrom.*, 1998, **9**, 1248.

6 P. D. Compton, *et al.*, *Anal. Chem.*, 2011, **83**, 6868.

7 S. K. Chowdhury, V. Katta and B. T. Chait, *J. Am. Chem. Soc.*, 1990, **112**, 9012.

8 (*a*) A. T. Iavarone, J. C. Jurchen and E. R. Williams, *J. Am. Soc. Mass Spectrom.*, 2000, **11**, 9; (*b*) M. H. Amad, *et al.*, *J. Mass Spectrom.*, 2000, **35**, 784.

9 (*a*) A. T. Iavarone and E. R. Williams, *J. Am. Chem. Soc.*, 2003, **125**, 8; (*b*) J. A. Loo, H. R. Udseth and R. D. Smith, *Biol. Mass Spectrom.*, 1988, **17**, 411.
10 D. Duft, *et al.*, *Nature*, 2003, **421**, 128.
11 M. Dole, *et al.*, *J. Chem. Phys.*, 1968, **49**, 2240.
12 (*a*) P. Kebarle and L. Tang, *Anal. Chem.*, 1993, **65**, 972A; (*b*) J. V. Iribarne and B. A. Thomson, *J. Chem. Phys.*, 1976, **64**, 2287; (*c*) J. Fernandez de la Mora, *Anal. Chim. Acta*, 2000, **406**, 11.
13 S. Zhou, B. S. Prebyl and K. D. Cook, *Anal. Chem.*, 2002, **74**, 4885.
14 C. L. Gatlin and F. Turecek, *Anal. Chem.*, 1994, **66**, 712.
15 T. R. Covey, *et al.*, *Rapid Commun. Mass Spectrom.*, 1988, **2**, 249.
16 U. A. Mirza and B. T. Chait, *Anal. Chem.*, 1994, **66**, 2898.
17 (*a*) H. J. Sterling, *et al.*, *Anal. Chem.*, 2012, **84**, 3795; (*b*) Y. Li and R. B. Cole, *Anal. Chem.*, 2003, **75**, 5739.
18 (*a*) P. D. Schnier, D. S. Gross and E. R. Williams, *J. Am. Soc. Mass Spectrom.*, 1995, **6**, 1086; (*b*) P. D. Schnier, D. S. Gross and E. R. Williams, *J. Am. Chem. Soc.*, 1995, **117**, 6747; (*c*) E. R. Williams, *J. Mass Spectrom.*, 1996, **31**, 831.
19 (*a*) S. K. Chowdhury, *et al.*, *J. Am. Soc. Mass Spectrom.*, 1990, **1**, 382; (*b*) Y. Cai and R. B. Cole, *Anal. Chem.*, 2002, **74**, 985; (*c*) S. D. Friess, *et al.*, *Int. J. Mass Spectrom.*, 2002, **219**, 269; (*d*) Y. Jiang and R. B. Cole, *J. Am. Soc. Mass Spectrom.*, 2005, **16**, 60; (*e*) T. G. Flick, S. I. Merenbloom and E. R. Williams, *J. Am. Soc. Mass Spectrom.*, 2011, **22**, 1968.
20 C. J. Krusemark, *et al.*, *J. Am. Soc. Mass Spectrom.*, 2009, **20**, 1617.
21 A. Kharlamova, *et al.*, *Anal. Chem.*, 2010, **82**, 7422.
22 (*a*) S. H. Lomeli, *et al.*, *J. Am. Soc. Mass Spectrom.*, 2010, **21**, 127; (*b*) H. J. Sterling, *et al.*, *J. Am. Soc. Mass Spectrom.*, 2011, **22**, 1178; (*c*) A. T. Iavarone, J. C. Jurchen and E. R. Williams, *Anal. Chem.*, 2001, **73**, 1455; (*d*) A. T. Iavarone and E. R. Williams, *Int. J. Mass Spectrom.*, 2002, **219**, 63; (*e*) S. G. Valeja, *et al.*, *Anal. Chem.*, 2010, **82**, 7515.
23 K. A. Douglass and A. R. Venter, *J. Am. Soc. Mass Spectrom.*, 2012, **23**, 489.
24 S. K. Sze, *et al.*, *Proc. Natl. Acad. Sci. U. S. A.*, 2002, **99**, 1774.
25 (*a*) S. M. Miladinovic, *et al.*, *Anal. Chem.*, 2012, **84**, 4647; (*b*) J. G. Meyer and E. A. Komives, *J. Am. Soc. Mass Spectrom.*, 2012, **23**, 1390.
26 R. R. Ogorzalek Loo, R. Lakshmanan and J. A. Loo, *J. Am. Soc. Mass Spectrom.*, 2014, **25**, 1675.
27 R. L. Grimm and J. Beauchamp, *J. Phys. Chem. A*, 2009, **114**, 1411.
28 M. Samalikova, *et al.*, *Anal. Bioanal. Chem.*, 2004, **378**, 1112.
29 C. A. Teo and W. A. Donald, *Anal. Chem.*, 2014, **86**, 4455.
30 W. A. Donald, G. N. Khairallah and R. A. J. O'Hair, *J. Am. Soc. Mass Spectrom.*, 2013, **24**, 811.
31 M. Graf, R. G. García and H. Wätzig, *Electrophoresis*, 2005, **26**, 2409.
32 S. A. McLuckey, G. J. Van Berkel and G. L. Glish, *J. Am. Chem. Soc.*, 1990, **112**, 5668.
33 W. M. Haynes, *CRC Handbook of Chemistry and Physics*, Taylor & Francis, 95th edn, 2014.
34 X. Liu and R. B. Cole, *J. Am. Soc. Mass Spectrom.*, 2011, **22**, 2125.
35 E. P. L. Hunter and S. G. Lias, *J. Phys. Chem. Ref. Data*, 1998, **27**, 413.
36 (*a*) C. A. Cassou and E. R. Williams, *Anal. Chem.*, 2014, **86**, 1640; (*b*) Y. Zhang and P. S. Cremer, *Curr. Opin. Chem. Biol.*, 2006, **10**, 658; (*c*) M. Hou, R. Lu and A. Yu, *RSC Adv.*, 2014, **4**, 23078.
37 D. N. Mortensen and E. R. Williams, *Anal. Chem.*, 2014, **86**, 9315.
38 N. J. Greenfield, *Nat. Protoc.*, 2006, **1**, 2876.
39 (*a*) H. J. Sterling and E. R. Williams, *J. Am. Soc. Mass Spectrom.*, 2009, **20**, 1933; (*b*) O. M. Hamdy and R. R. Julian, *J. Am. Soc. Mass Spectrom.*, 2012, **23**, 1.
40 E. V. Anslyn and D. A. Dougherty, *Modern Physical Organic Chemistry*, University Science, USA, 2006, p. 259.
41 D. M. Horn, R. A. Zubarev and F. W. McLafferty, *Proc. Natl. Acad. Sci. U. S. A.*, 2000, **97**, 10313.
42 H. J. Sterling and E. R. Williams, *Anal. Chem.*, 2010, **82**, 8.